can obtain an exact solution from the equations of this Note as easily by using the same tables. Therefore, these exact equations are recommended.

References

[1] Mascitti, V. R., "Charts of Additive Drag Coefficient and Mass-Flow Ratio For Inlets Utilizing Right Circular Cones at Zero Angle of Attack," TN D-3434, 1966, NASA.

[2] Barry, F. W., "Conical Flow Properties for Use in the Design of Supersonic Inlets," Rept. M-1266-1, 1958, UAC Research Dept., East Hartford, Conn.

[3] Sims, J. L., "Tables for Supersonic Flow Around Right Circular Cones at Zero Angle of Attack," SP-3004, 1964, NASA.

[4] Mascitti, V. R., "An Approximate Solution of Additive-Drag Coefficient and Mass-Flow Ratio For Inlets Utilizing Right Circular Cones at Zero Angle of Attack," TN-5537, 1969, NASA.

Wave Structure of Exhaust from Transonic Aircraft

ALLEN E. FUHS*

Air Force Aero Propulsion Laboratory (AFSC), Wright-Patterson Air Force Base, Ohio

IN the discussion of jets exhausting into a moving airstream Pindzola,[1] Ehlers and Strand,[2] and Kawamura[3] use a reflection coefficient k which assumes a value of unity for no reflection. Waldman and Probstein[4] and Hayes and Probstein[5] use a reflection coefficient R which has a value of zero for no reflection. Using R to interpret inviscid jets, one can draw a map in the $M_j - M_\infty$ plane which is of value for understanding aircraft exhausts.

Figure 1 shows the geometry of the reflection at a shear layer. The two reflection coefficients are defined as

$$R = (p_5 - p_4)/(p_4 - p_3) \tag{1}$$

and

$$k = (p_{14} + p_{24} - 2)/(p_{14} - p_{24}) \tag{2}$$

Here p_{14} is ratio of p_1 to p_4; this is standard notation. In terms of the flow properties the reflection coefficients are given by

$$k = Y_j/Y_\infty \tag{3}$$

and

$$R = (Y_\infty - Y_j)/(Y_\infty + Y_j) \tag{4}$$

where the dimensionless quantity Y is

$$Y = \gamma M^2/(M^2 - 1)^{1/2} \tag{5}$$

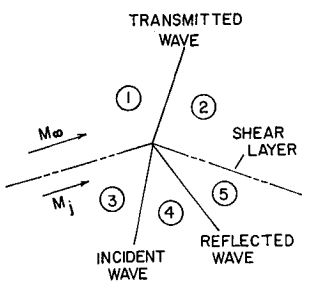

Fig. 1 Geometry of reflection at a shear layer.

Received October 15, 1970.

* Chief Scientists; now Professor, Department of Aeronautics, Naval Postgraduate School, Monterey, Calif. Associate Fellow AIAA.

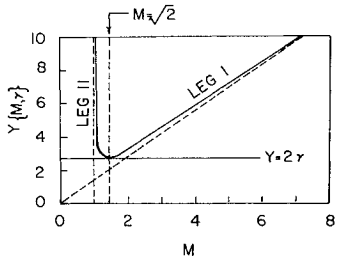

Fig. 2 Curve of Y vs M for $\gamma = 1.4$.

Figure 2 shows the behavior of Y, and it is this behavior that makes for varied jet phenomena in the transonic region. As can be seen from Eq. (4), it is the relative size of Y_∞ and Y_j which determines the algebraic sign of the reflection coefficient R. If R is negative then the reflected wave is the opposite of the incident wave, i.e., an incident compression wave is reflected as an expansion wave.

We are all familiar with the train of shock diamonds that occur from an underexpanded jet. Pictures of static test firing of rockets will show a half dozen or more. Also pictures of exhaust from afterburning turbojets† show similar patterns. In order to have the periodic jet structure it is necessary to have a negative reflection coefficient. The jet must expand, compress, expand, compress, etc. When R is positive for an underexpanded jet there is expansion by fans originating at nozzle exit lip, recompression by imbedded jet shock and then expansion to atmospheric pressure. There is no repetition of the wave pattern.

For a periodic jet, the streamline dividing the jet from the ambient air stream takes on a shape like a corrugated cylinder. For a nonperiodic jet the dividing streamline simply diverges if the jet shock is strong or converges and then diverges once if jet shock is weak. Of course, viscous effects tend to wash out the wave pattern. Even so there remains a different character between the two jets formed with R positive and R negative.

Figure 3 shows the map, which was mentioned earlier, of the different regions for the reflection coefficient. This map is obtained from Eq. (4) along with use of Fig. 2. In the region bounded by $(2)^{1/2} < M_j < \infty$ and $(2)^{1/2} < M_\infty < \infty$ both Y_j and Y_∞ are on leg I of Fig. 2. In the region bounded by $1 < M_j < (2)^{1/2}$ and $1 < M_\infty < (2)^{1/2}$ both Y_j and Y_∞ are on leg II. In other regions Y_j and Y_∞ are on different legs. The curve in Fig. 3 labeled curve A is obtained from the solution of $Y_j = Y_\infty$.

For illustration purposes consider a fixed M_∞ which is represented by dashed line in Fig. 3. Now consider the change in jet character as engine pressure ratio changes resulting in changed M_j. From 1 to 2 the jet is periodic; from 2 to 3 it is nonperiodic and once again from point 3 toward higher M_j the jet is periodic. Over a fairly narrow Mach number range of either M_∞ or M_j the jet undergoes pronounced change in wave structure.

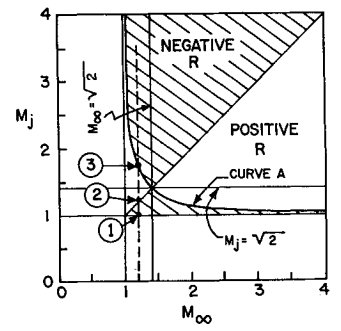

Fig. 3 Map of reflection coefficient in $M_\infty - M_j$ plane.

† Due to volume and weight constraints both rockets and turbojets tend to operate underexpanded.

The use of reflection coefficient R in place of k provides more insight to jet wave patterns and permits one to draw a neat map in $M_j - M_\infty$ plane.

References

[1] Pindzola, M., "Jet Simulation in Ground Test Facilities," AGARDograph 79, Nov. 1963.

[2] Ehlers, F. E. and Strand, T., "The Flow of a Supersonic Jet in a Supersonic Stream at Angle of Attack," *Journal of the Aerospace Sciences*, Vol. 25, 1958, p. 497.

[3] R. Kawamura, "Reflection of a Wave at an Interface of Supersonic Flows and Wave Patterns in a Supersonic Compound Jet," *Journal of the Physical Society of Japan*, Vol. 7, Sept.-Oct. 1952.

[4] Waldman, R. and Probstein, R. F., "An Analytical Extension of the Shock Expansion Method," *Journal Aerospace of the Sciences*, Vol. 28, 1961, p. 119.

[5] Hayes, W. D. and Probstein, R. F., *Hypersonic Flow Theory*, Academic Press, New York, 1959.

Development of a Gliding Guided Ribbon Parachute for Transonic Speed Deployment

WILLIAM B. PEPPER* AND IRA T. HOLT†
Sandia Laboratories, Albuquerque, N. Mex.

Introduction

PARACHUTE retardation is often a necessity on some drop vehicles to help control performance and trajectory. With the increased time of fall, dispersion suffers from unknown winds. A guided parachute system could be used to improve accuracy in many applications.

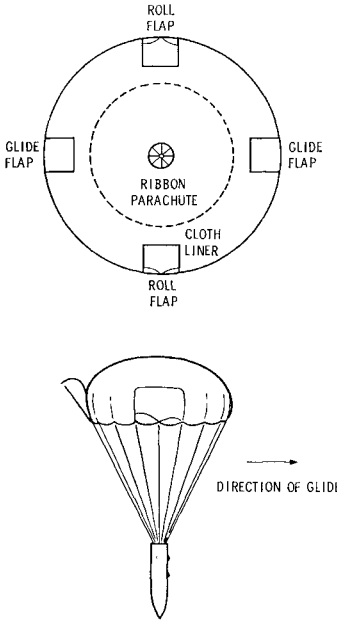

Fig. 1 Sketch of gliding ribbon parachute.

Received August 10, 1970; revision received October 15, 1970. This work was supported by the U.S. Atomic Energy Commission.

* Project Leader, Rocket and Recovery Systems Division, Aerothermodynamics Projects Department. Associate Fellow AIAA.

† Member of Technical Staff, Rocket and Recovery Systems Division, Aerothermodynamics Projects Department.

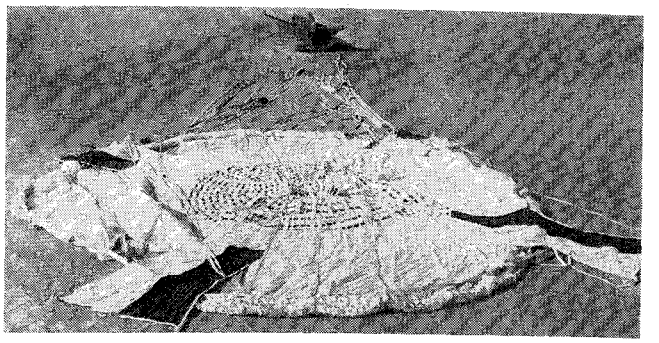

Fig. 2 Gliding parachute after drop test at Tonopah Test Range, Nevada.

Earlier work with guided parachutes at Sandia was done with solid chutes with one gore missing,[1] or with the parafoil.[2] Both of these systems were suited for low-speed deployments only. To develop a system for higher-speed deployments, recent research has been directed at using conventional ribbon parachutes,[3] modified to provide a glide and turn capability without materially affecting opening reliability, structural integrity, or effective drag.

Parachute Design

The system presently being tested consists of a standard heavy duty flat circular 24-ft diam, 32-gore, ribbon parachute that has been modified, as shown in Fig. 1, for controlled gliding flight. The canopy has been lined on the inner side from the skirt band up radially for 5 ft with 1.6 oz/yd^2 nylon cloth. Two glide flaps, 2 gores wide and 5 ft high, have been made diametrically opposite each other. These flaps are interconnected so that as one opens, the other closes, and for neutral glide, they are each half open. This way, either forward or backward glide can be commanded.

Roll control is obtained by making two roll flaps on the skirt located 90° from the glide flaps. Most effective control has been obtained by the "butterfly" arrangement shown. Again, the flaps are interconnected so that as the clockwise portion of both flaps close, the counterclockwise portions open. At neutral roll, all four portions are half open. When the portions that are physically located on the clockwise sides are open, the system will roll counterclockwise.

Development

The system has been developed by wind-tunnel testing,[4] vehicle tow tests, and full scale drop tests. Wind-tunnel tests were conducted to investigate gliding performance. Several combinations of glide flap size and amount of flap movement were tested. Ribbon canopies with differing amounts of a solid inner lining were also tried. From a visual analysis and determination of the zero moment point, the results indicated a glide angle of 25° off the vertical could be obtained. Cloth lining in the skirt area of ribbon chutes was found to increase glide capability.

Drop tests using the 24-ft chute and a 2500-lb vehicle, shown in Fig. 2, were conducted from a C-54 aircraft at the instrumented AEC Tonopah Test Range, Nevada, and the predicted glide angle of approximately 25° was verified.

Radio-controlled flights were then made using two motors to open and close the flaps on command. Each motor drives a windlass wound to reel out one line while pulling in another. One windlass is attached to both glide flaps, and the other is attached to both roll flaps. Using reversible motors, both forward and reverse glide and clockwise and counterclockwise roll can be obtained. The parachute and vehicle after drop test are shown in Fig. 2.

The "bang-bang" type of control originally employed caused stability problems by forcing full glide too fast, making it difficult to hold a given heading; therefore, proportional